Detection sensitivity of laser feedback interferometry using a terahertz quantum cascade laser

J. Keeley,[1,*] K. Bertling,[2] P. L. Rubino,[1] Y. L. Lim,[2] T. Taimre,[3] X. Qi,[2] I. Kundu,[1] L. H. Li,[1] D. Indjin,[1] A. D. Rakić,[2] E. H. Linfield,[1] A. G. Davies,[1] J. Cunningham,[1] and P. Dean[1]

[1]*School of Electronic & Electrical Engineering, University of Leeds, Leeds, LS6 9JT, England, United Kingdom*
[2]*School of Information Technology and Electrical Engineering, The University of Queensland, St Lucia, QLD 4072, Australia*
[3]*School of Mathematics and Physics, The University of Queensland, St Lucia, QLD 4072, Australia*
Corresponding author: j.t.keeley@leeds.ac.uk

We report on the high detection sensitivity of a laser feedback interferometry scheme based on a terahertz frequency quantum cascade laser (QCL). We show that variations on the laser voltage induced by optical feedback to the laser can be resolved with the reinjection of powers as low as ~ – 125 dB of the emitted power. Our measurements demonstrate a noise equivalent power of ~1.4 pW/$\sqrt{\text{Hz}}$, although, after accounting for the reinjection losses, we estimate that this corresponds to only ~1 fW/$\sqrt{\text{Hz}}$ being coupled to the QCL active region.

The effects of optical feedback (OF) in laser systems have been observed since the early days of laser development [1]. While OF can result in undesirable and unpredictable operation in lasers, it can also be harnessed for metrological purposes. Indeed, there has been significant interest recently in laser feedback interferometry (LFI) which utilizes the "self-mixing" (SM) effect in lasers [2], with particular interest in the use of quantum cascade laser (QCL) sources for coherent imaging and sensing applications at terahertz (THz) frequencies [3–9]. By exploiting the perturbation to the laser voltage induced under OF, these approaches offer the prospect of compact THz systems with ultrafast response times that circumvent the reliance on cryogenically cooled or slow room-temperature THz detectors. Yet, among the emerging applications of such systems, there is an increasing demand for high detection sensitivities that can rival those of commercial cryogenically cooled THz detectors. One notable example is THz scattering scanning near-field optical microscopy (THz-s-SNOM) [10,11], which

relies on the detection of radiation scattered weakly from the tip of a nanometric needle probe held in proximity to a sample. Through this approach, imaging resolutions far beyond the diffraction limit ($< \lambda/1000$) can be obtained. However, the scattering cross section of the needle tip scales with the diameter of the tip apex and, as such, the noise equivalent power (NEP) of the detection system can ultimately limit the highest resolution attainable. Similarly, for gas spectroscopy and sensing applications exploiting LFI in THz QCLs [12,13], the NEP influences the maximum extinction coefficient that can be measured. In this Letter, we investigate experimentally the detection sensitivity of the LFI scheme in a THz QCL and demonstrate a NEP of ~1.4 pW/$\sqrt{\text{Hz}}$ without accounting for reinjection losses—a value comparable to that achievable with commercial cryogenically cooled THz detectors.

Our LFI scheme is based on simple reflection geometry, as shown in Fig. 1, in which a movable planar mirror reinjects radiation to the laser facet, forming an external cavity of length $L \approx 0.48$ m. The QCL used in this Letter consisted of a 14 μm thick GaAs/AlGaAs 9-well active region emitting at a frequency of ~3.4 THz [14]. The device was processed into a semi-insulating surface-plasmon ridge waveguide with dimensions of 2.9 mm × 150 μm, which was cooled to a temperature of 25 K using a continuous-flow helium cryostat. The QCL was operated with a continuous driving current of 400 mA, just above the lasing threshold of 380 mA, where the SM voltage signal is greatest with no additional external cavity attenuation (see Fig. 1 inset) [4]. At this driving current, the emitted power, measured at the external planar mirror using a calibrated THz power meter, was found to be ~22.4 μW. OF to the laser was modulated at a frequency $f_{mod} \approx 200$ Hz using a mechanical chopper [15], and the SM signal V_{SM} was monitored via the laser terminal voltage using a lock-in amplifier referenced to f_{mod}. Interferometric variations on the terminal voltage were recorded by extending the external cavity over a distance of 200 μm in steps of 4 μm, with the SM voltage signal, V_{SM}, being recorded at each mirror position. This cavity
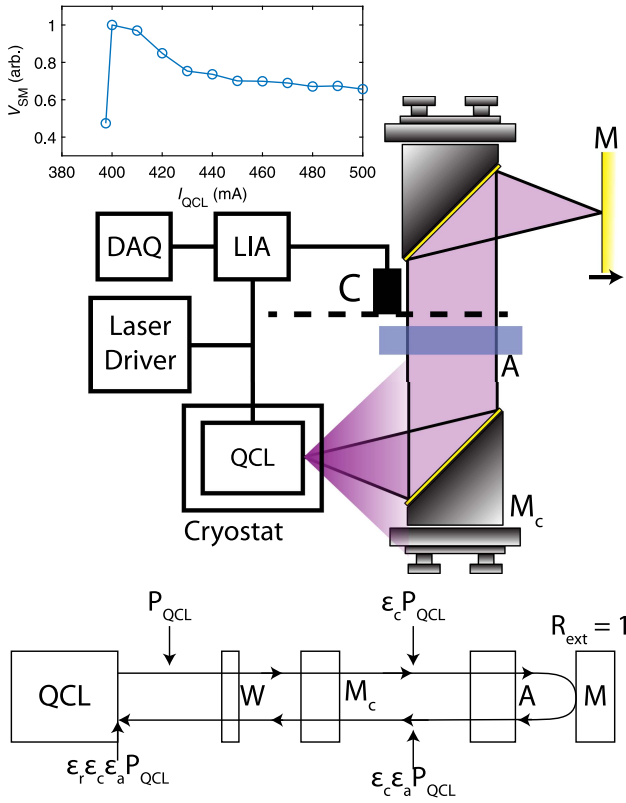
Fig. 1. Experimental system for measuring the detection sensitivity of LFI based on a THz QCL. LIA, lock-in amplifier; DAQ, digital acquisition; C, mechanical chopper; A, THz attenuators; W, cryostat window; M_c, collection mirror; M, movable planar mirror. Inset, SM voltage signal V_{SM} as a function of driving current with no additional external cavity attenuation. Bottom, radiation path showing THz power at each position. The power attenuation coefficients ε_a, ε_c, and ε_r are defined in the text.

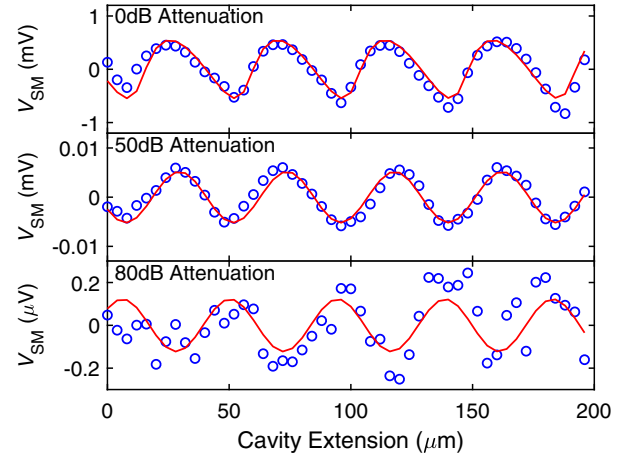**Fig. 2.** Interferometric waveforms measured for an external cavity extension of 200 µm under various levels of double-pass power attenuation ε_a. Also shown (red lines) are fits to Eq. (1).

extension is far below the Rayleigh length of our optical system (~1.8 mm), ensuring that beam focusing has a negligible effect on our measurements. In contrast to previous measurements of the minimum detectable power [16], the use of lock-in detection in this Letter can be expected to provide several orders of magnitude improvement.

In this scheme, the response of the QCL can be described using the steady-state solution of the model proposed by Lang and Kobayashi [17]. This predicts a modulation of the laser terminal voltage described by the relation [18]

$$V_{SM} \propto \sqrt{\varepsilon_a \varepsilon_c \varepsilon_r} \sqrt{R_{ext}} \cos\left(\frac{2L\omega}{c}\right), \tag{1}$$

where L is the cavity length formed by the external mirror with reflectance R_{ext}, ω is the angular emission frequency under OF, and c is the speed of light. The power attenuation factor ε_c is a coupling constant inherent to the optical system that accounts for loss due to imperfect collection of the radiation emitted from the laser by the F/2 parabolic collection mirror, including loss due to imperfect transmission through the cryostat window. From measurements of the power at both the cryostat window and at the external planar mirror, we determine the collection losses in our system to be $\varepsilon_c \sim -10$ dB. The power attenuation factor ε_r represents the reinjection loss between the

external planar mirror and the laser cavity, including the loss due to transmission through the cryostat window, and spatial mode mismatch between the reflected and cavity modes. The power attenuation factor ε_a is a coupling constant accounting for additional attenuation introduced to the external cavity. In our experiment, ε_a was controlled by introducing calibrated THz power attenuators in the external cavity, which provided a double-pass attenuation in the range $\varepsilon_a = 0$ to -90 dB. This allowed the maximum tolerable additional cavity attenuation to be determined, as the level of attenuation where interferometric variations on the laser terminal voltage were reduced to the voltage noise level.

Figure 2 shows the SM voltage interferograms recorded with a 10 s time constant (equivalent detection bandwidth ~0.025 Hz), for varying degrees of additional cavity attenuation. The non-sinusoidal form of these interferograms is a result of ω in Eq. (1) being dependent on the external cavity length, as described by the excess phase equation [2,17,19]. The magnitude of this perturbation to the lasing frequency under OF is also dependent on the feedback parameter C, defined as

$$C = \frac{\tau_{ext}}{\tau_L} \sqrt{1 + \alpha^2} \kappa, \tag{2}$$

where τ_{ext} is the round-trip time in the external cavity, τ_L is the laser round-trip time, α is the linewidth enhancement factor, and the dimensionless feedback coupling coefficient κ is related to the attenuation coefficients ε_a, ε_c, and ε_r, and the reflectances of the laser emission facet, R_2, and external target, R_{ext}, according to the relationship

$$\kappa = \sqrt{\varepsilon_a \varepsilon_c \varepsilon_r}(1 - R_2)\sqrt{\frac{R_{ext}}{R_2}}. \tag{3}$$

Also shown in Fig. 2 are fits of the data to Eq. (1). In the case of $\varepsilon_a = 1$ (i.e. with no additional attenuation in the external cavity) we determine values $C = 0.39$ and $\alpha = -1.92$ from the fit to our data. Using the excess phase equation [2,17,19] this value of C predicts a small change in lasing frequency of only ~19 MHz under OF. Although values of α in the range ~−0.1 to ~0.5 are typically obtained from THz QCLs based on a bound-to-continuum active region
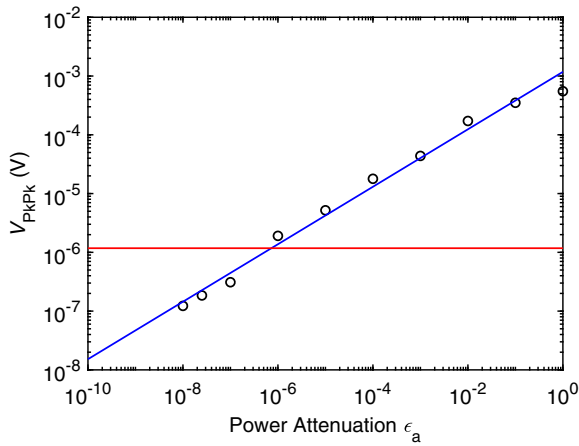
Fig. 3. Peak-to-peak values of the SM voltage interferograms, V_{PkPk}, as a function of additional power attenuation introduced in the external cavity, ε_a. The horizontal line indicates the voltage noise floor in our system at a level $\sim 1.5~\mu V/\sqrt{Hz}$.

Table 1. Fitting Parameters and Estimated Values of the Minimum Detectable Reinjected Power Obtained from Measurements with Different External Attenuations ε_a

ε_a (dB)	C	$\sqrt{\varepsilon_c \varepsilon_r}$	ε_r (dB)	Reinjected power (fW/$\sqrt{Hz}$)
0	0.39	0.0033	−39.5	0.16
−10	0.24	0.0063	−34.0	0.56
−20	0.13	0.0112	−28.9	1.81
−30	0.03	0.0086	−31.3	1.04

design [16,20], we note that values deviating significantly from this range have been reported elsewhere [3] for active regions with phonon-assisted electron injection, such as that employed in this Letter.

Figure 3 shows the peak-to-peak values of the SM voltage interferograms, V_{PkPk}, determined from the fits to the data shown in Fig. 2, plotted as a function of additional power attenuation in the cavity; a linear relationship between $\sqrt{\varepsilon_a}$ and V_{PkPk} can be established, as expected from Eq. (1). Also shown in Fig. 3 is the voltage noise floor in our system, which is dominated by current noise in the laser driver. Other sources of noise in our system, such as the input noise of the lock-in amplifier are on the order of $\sim nV/\sqrt{Hz}$, far below the laser driver noise.

As can be seen, variations on the laser voltage can be resolved with up to $\sim$−80 dB of additional attenuation introduced in the external cavity. Based on the power measured in the external cavity, and without accounting for reinjection losses, this measurement corresponds to a detection NEP of $\sim 1.4~pW/\sqrt{Hz}$.

By estimating the reinjection losses in our system, it is possible to estimate the corresponding minimum detectable power coupled coherently to the laser active region. Firstly, using the fitted values for C and α in Eq. (2), and assuming $R_{ext} = 1$ for the gold mirror and $R_2 = 0.32$ for the laser facet, we can estimate the attenuation factor $\varepsilon_c \varepsilon_r$ for our optical system via Eq. (3). By accounting for the measured value $\varepsilon_c \sim$ −10 dB, we can thus obtain an estimate of ε_r. Table 1 summarizes the results of this analysis for each of the four measurements up to −30 dB of additional cavity attenuation; we note that the small values of C ($\ll 0.1$) resulting from greater attenuation ($\varepsilon_a <$ −30 dB) cannot be obtained reliably from the fitting procedure. The reinjection losses shown in Table 1 arise primarily from coherent coupling of the returning field to the laser cavity. Indeed, the spot size of the returning beam focused on the laser facet is expected to be on the order $\sim 250~\mu m$ [4], far larger than the 14 μm × 150 μm facet of the laser active region. We also note that the variation in ε_r between measurements can be explained by the fact that the insertion of attenuators in the external cavity can change the divergence

angle of the propagating field. As such, the attenuation ε_r cannot be assumed to act independently to ε_a. Nevertheless, from our measured NEP of $\sim 1.4~pW/\sqrt{Hz}$, we can obtain the reinjected power for each of these four measurements. Based on these results (see Table 1) we can estimate that our NEP corresponds to only $\sim 1~fW/\sqrt{Hz}$ being coupled coherently to the laser active region. As such, improvements in the coupling to the active region could in principle lead to further improvement in the NEP.

Finally, it is interesting to evaluate the intrinsic limit for the maximum tolerable power attenuation for our QCL source, and to compare this figure with our measured value. It can be expected that OF induces a non-negligible effect on the operating parameters of a laser when the rate of the photon reinjection to the cavity exceeds the rate of spontaneous emission in the cavity [21].

Using a recently reported reduced rate equation model of a THz QCL under OF, this condition can be expressed as [22]

$$\frac{2\kappa}{\tau_L} S > \frac{M\beta_{sp}N_3}{\tau_{sp}}, \qquad (4)$$

where S is the photon number, M is the number of periods in the QCL active region, β_{sp} is the spontaneous emission factor, N_3 is the upper lasing level carrier number, and τ_{sp} is the spontaneous emission lifetime.

By evaluating Eqs. (3) and (4) using typical values for our QCL device [22] (see Table 2), we predict an intrinsic limit for the maximum tolerable total power attenuation equal to $\sim$−150 dB, which is in reasonable agreement with the experimentally determined value of $\varepsilon_a \varepsilon_c \varepsilon_r \sim$ −(80 + 10 + 35) = −125 dB. The discrepancy between these values can be attributed to voltage noise in our system, which is dominated by the laser driver and could be reduced through the use of a more stable current source, for example, a dc battery. As a final point, we can compare this figure to that expected for a mid-infrared QCL. Using typical parameter values [23], we predict a maximum tolerable total power attenuation of only $\sim$−134 dB in

Table 2. QCL Device Parameters Used to Predict the Maximum Tolerable Total Power Attenuation in LFI [22]

R_{ext}	1
R_2	0.324
M	117
β_{sp}	1.63×10^{-4}
N_3	1.07×10^{7}
τ_{sp}	5.1×10^{-6} s
τ_L	7.04×10^{-11} s
S	3.69×10^{7}

this case. This lower value is primarily a result of smaller spontaneous emission lifetime in the mid-infrared QCL.

In this Letter, the detection sensitivity of an LFI scheme based on a THz-frequency QCL has been quantified. Our measurements demonstrate that variations on the laser voltage induced by OF to the laser can be resolved with the reinjection of powers as low as ~-125 dB of the emitted power, composing ~45 dB of losses inherent to the optical system and an additional 80 dB of power attenuation introduced in the external cavity. This corresponds to a NEP for our scheme of ~1.4 pW/$\sqrt{\text{Hz}}$, or a minimum detectable power of 2.2 pW for a time constant of 100 ms (equivalent detection bandwidth ~2.5 Hz). By considering the reinjection losses, we estimate this corresponds to only ~1 fW/$\sqrt{\text{Hz}}$ being coupled coherently to the laser active region. This Letter demonstrates the high suitability of the LFI scheme to applications that require the detection of weakly scattered THz radiation, such as THz-s-SNOM.

REFERENCES

1. D. A. Kleinman and P. P. Kisliuk, Bell Sys. Tech. J. **41**, 453 (1962).
2. R. Kliese, T. Taimre, A. A. A. Bakar, Y. L. Lim, K. Bertling, M. Nikolić, J. Perchoux, T. Bosch, and A. D. Rakić, Appl. Opt. **53**, 3723 (2014).
3. M. Wienold, T. Hagelschuer, N. Rothbart, L. Schrottke, K. Biermann, H. Grahn, and H.-W. Hübers, Appl. Phys. Lett. **109**, 011102 (2016).
4. P. Dean, Y. L. Lim, A. Valavanis, R. Kliese, M. Nikolić, S. P. Khanna, M. Lachab, D. Indjin, Z. Ikonić, P. Harrison, A. D. Rakić, E. H. Linfield, and A. G. Davies, Opt. Lett. **36**, 2587 (2011).
5. F. P. Mezzapesa, L. L. Columbo, M. Brambilla, M. Dabbicco, M. S. Vitiello, and G. Scamarcio, Appl. Phys. Lett. **104**, 041112 (2014).
6. Y. Ren, R. Wallis, D. S. Jessop, R. DeglInnocenti, A. Kilmont, H. E. Beere, and D. A. Ritchie, Appl. Phys. Lett. **107**, 011107 (2015).
7. J. Keeley, J. Freeman, K. Bertling, Y. L. Lim, R. A. Mohandas, T. Taimre, L. H. Li, D. Indjin, A. D. Rakić, E. H. Linfield, A. G. Davies, and P. Dean, Sci. Rep. **7**, 7236 (2017).
8. Y. L. Lim, T. Taimre, K. Bertling, P. Dean, D. Indjin, A. Valavanis, S. P. Khanna, M. Lachab, H. Schaider, T. W. Prow, H. P. Soyer, S. J. Wilson, E. H. Linfield, A. G. Davies, and A. D. Rakić, Biomed. Opt. Express **5**, 3981 (2014).
9. Y. L. Lim, K. Bertling, T. Taimre, T. Gillespie, C. Glenn, A. Robinson, D. Indjin, Y. Han, L. Li, E. H. Linfield, A. G. Davies, P. Dean, and A. D. Rakić, Opt. Express **27**, 10221 (2019).
10. R. DeglInnocenti, R. Wallis, B. Wei, L. Xiao, S. J. Kindness, O. Mitrofanov, P. Braeuningerm-Weimer, S. Hofmann, H. E. Beere, and D. A. Ritchie, ACS Photonics **4**, 2150 (2017).
11. P. Dean, O. Mitrofanov, J. Keeley, I. Kundu, L. Li, E. H. Linfield, and A. G. Davies, Appl. Phys. Lett. **108**, 091113 (2016).
12. R. Chhantyal-Pun, A. Valavanis, J. T. Keeley, P. Rubino, I. Kundu, Y. Han, P. Dean, L. Li, A. G. Davies, and E. H. Linfield, Opt. Lett. **43**, 2225 (2018).
13. T. Hagelschuer, M. Wienold, H. Richter, L. Schrottke, H. T. Grahn, and H.-W. Hbers, Opt. Express **25**, 30203 (2017).
14. M. Wienold, L. Schrottke, M. Giehler, R. Hey, W. Anders, and H. Grahn, Electron. Lett. **45**, 1030 (2009).
15. K. Bertling, T. Taimre, G. Agnew, Y. L. Lim, P. Dean, D. Indjin, S. Hofling, R. Weih, M. Kamp, M. von Edlinger, J. Koeth, and A. D. Rakić, IEEE Sens. J. **16**, 1937 (2016).
16. Y. L. Lim, P. Dean, M. Nikoli, R. Kliese, S. P. Khanna, M. Lachab, A. Valavanis, D. Indjin, Z. Ikoni, P. Harrison, E. H. Linfield, A. G. Davies, S. J. Wilson, and A. D. Rakić, Appl. Phys. Lett. **99**, 081108 (2011).
17. R. Lang and K. Kobayashi, IEEE J. Quantum Electron. **16**, 347 (1980).
18. K. Petermann, Laser Diode Modulation and Noise (Springer, 1988).
19. T. Taimre, M. Mikoli, K. Bertling, Y. Lim, T. Bosch, and A. Rakić, Adv. Opt. Photonics **7**, 570 (2015).
20. R. P. Green, J.-H. Xu, L. Mahler, A. Tredicucci, F. Beltram, G. Giuliani, H. E. Beere, and D. A. Ritchie, Appl. Phys. Lett. **92**, 071106 (2008).
21. G. P. Agrawal and N. K. Dutta, Semiconductor Lasers (Springer, 1995).
22. G. Agnew, A. Grier, T. Taimre, Y. L. Lim, K. Bertling, Z. Ikoni, A. Valavanis, P. Dean, J. Cooper, S. P. Khanna, M. Lachab, E. H. Linfield, A. G. Davies, P. Harrison, D. Indjin, and A. D. Rakić, Opt. Express **24**, 20554 (2016).
23. A. Hamadou, S. Lamari, and J.-L. Thobel, J. Appl. Phys. **105**, 093116 (2009).
24. Dataset for graphs in figures 1, 2, 3, https://doi.org/10.5518/589.